

## Current Flows in Pulsar Magnetospheres \*

Ren-Xin Xu, Xiao-Hong Cui and Guo-Jun Qiao

Department of Astronomy, School of Physics, Peking University, Beijing 100871;  
[r.x.xu@pku.edu.cn](mailto:r.x.xu@pku.edu.cn)

Received 2005 July 19; accepted 2005 October 19

**Abstract** The global structure of current flows in pulsar magnetosphere is investigated, with rough calculations of the circuit elements. It is emphasized that the potential of the *critical field lines* (the field lines that intersect the null surface at the light cylinder radius) should be the same as that of interstellar medium, and that pulsars whose rotation axes and magnetic dipole axes are parallel should be positively charged, in order to close the pulsar's current flows. The statistical relation between the radio luminosity and pulsar's electric charge (or the spindown power) may hint that the millisecond pulsars could be low-mass bare strange stars.

**Key words:** pulsars: general — stars: neutron — dense matter

### 1 INTRODUCTION

Since Hewish et al. (1968) discovered the first radio pulsar, more and more magnetospheric models for pulsars have been proposed to explain their observed features. The vacuum inner gap model, on the one hand, suggested first by Ruderman & Sutherland (1975, hereafter RS75) depends on enough binding energy of charged particles on the pulsar surface (Wang et al. 2003). Qiao et al. (2004a) noted that the pulsar polar region can be divided into two parts by *the critical field line* (the field lines that intersect the null surface at the light cylinder radius, RS75) and suggested that the conventional inner core gap (ICG) and the inner annular gap (IAG) could be formed above the central and annular polar regions, respectively. The coexistence of both regions can well interpret the “bi-drifting” phenomenon in PSR J0815+09 (Qiao et al. 2004b). The space charge-limited flow model (e.g., Arons & Scharlemenn 1979; Harding & Muslimov 1998), on the other hand, is without any binding energy. An outer gap near the light cylinder has also been proposed (e.g., Cheng, Ho & Ruderman 1986), the existence of which may also reflect strong binding of particles on pulsar surface (Xu 2003a). However, even as observational data in radio, optical, X-ray, and  $\gamma$ -ray bands are being accumulated, there are still a great number of puzzles to be solved (e.g., Melrose 2004). Nevertheless, the models depend obviously on the nature of the pulsars surface; one may wish to draw conclusions on its interior structure (e.g., whether they are normal neutron stars or bare strange stars, see, e.g., Xu 2003b) through investigating of pulsar emission models. Note that it is almost impossible to concluded on the nature of pulsar via calculations in supranuclear physics.

The study of the pulsar magnetosphere is essential for us to understand various radiative processes, hence the observed emissions in different bands. Goldreich & Julian (1969) argued that a pulsar must have a *magnetosphere* with charge-separated plasma and demonstrated that a steady

---

\* Supported by the National Natural Science Foundation of China.

current would appear if charges can flow freely along the magnetic field lines from the pulsar surface. Sturrock (1971) pointed out that such a steady flow is impossible due to pair formation, and suggested that a simple electric circuit of the pulsar magnetosphere would be a discharge tube connected with an electromotive source. RS75 proposed that sparking process takes place in a charge-depletion gap just above the pulsar surface. The sparking points drift due to  $\mathbf{E} \times \mathbf{B}$ , which can naturally explain the drifting subpulse phenomena observed in radio band. Based on the assumption that the magnetosphere has a global current loop which starts from the star, runs through the outer gap, the wind and the inner gap, and returns to the star, Shibata (1991) proposed a circuit including an electromotive source connected in series with two accelerators (the inner and outer gaps) and a wind. Providing a fully general relativistic description, Kim et al. (2005) studied the pulsar magnetosphere and found that the direction of poloidal current in a neutron star magnetosphere is the same as that in a black hole.

In this work, assuming that the critical magnetic-field lines are at the same electric potential as the interstellar medium (ISM)<sup>1</sup> (Goldreich & Julian 1969), we propose a circuit model for the pulsar magnetosphere. For an *aligned* pulsar whose rotation axis is parallel to the magnetic axis, we find that the pulsar should be positively charged on the surface under the condition of the close circuit. The total electric field along the field line,  $E_{\parallel}$ , in the magnetosphere is then composed of two components: that due to charge-departure from the Goldreich-Julian density, and that due to the charge of the pulsar.

This paper is arranged as follows. The model is introduced in Section 2. The total charges of pulsar are estimated in Section 3. In Section 4, we discuss the charges of low-mass strange stars and present observational evidence for low-mass millisecond pulsars. Section 5 presents our conclusions.

## 2 THE MODEL

As shown in Figure 1, the foot points of the lines ‘a’, ‘b’, and the rotation axis on the star surface are denoted as Points ‘A’, ‘B’ and ‘P’. Point ‘P’ is also the magnetic pole of the star. We assume that the potential of the *critical field line b* equals to that of ISM at infinity,  $\phi_B = 0$ ; otherwise, a closed electric current in the two regions (i.e., *Region I*: bounded by lines “a”, and *Region II*: between lines ‘a’ and ‘b’) of open field lines is impossible.<sup>2</sup> Then for an *aligned* pulsar, the potential  $\phi_I < 0$  (within *Region I*) and  $\phi_{II} > 0$  (within *Region II*) in the regime of  $\phi_B = 0$ . Therefore, the negatively charged particles should flow out along the open magnetic field lines within *Region I* from the star, but positively charged particles flow out through *Region II*.

These flowing charged particles to the collimated direction form the current of a circuit. A circuit model can be proposed to describe the pulsar magnetosphere. The relation between the elements of the magnetosphere and circuit is as follows.

- (1) The total inner radiation of the pulsar corresponds to an electromotive power connected in parallel with a capacitor. Note that the resistance is negligible due to the perfect conductivity of the star.
- (2) The inner gaps which include the ICG and the IAG (Qiao et al. 2004a, 2004b) correspond to a parallel connection of a resistor and a capacitor. When a spark takes place in the gap, it can be represented by a resistor; if there is no spark, the voltage on the gap is so high that it can be described by a capacitor.
- (3) The outer gap and the pair-plasma wind correspond to a series connection of an inductor and a parallel connection of a resistor and a capacitor.

The inner gaps (including ICG and IAG in this paper) and an outer gap may work in a magnetosphere.<sup>3</sup> There is no current in the circuit until a spark takes place in the inner gaps, so

<sup>1</sup> We choose the potential of the ISM to be zero,  $\phi_{\text{ISM}} = 0$ .

<sup>2</sup> For *aligned* pulsars, electric current flows outward in the two regions if one sets the potential of the polar line to equal to that of ISM,  $\phi_P = 0$ , since all the potentials of open-field lines, except the polar line, are greater than zero. Also one can see that the current flows inward in those two regions if one chooses the potential of the last open-field lines to be zero,  $\phi_A = 0$ . Current flows can *not* be closed in both these cases.

<sup>3</sup> The inner annular gap and the outer gap might not exist simultaneously.

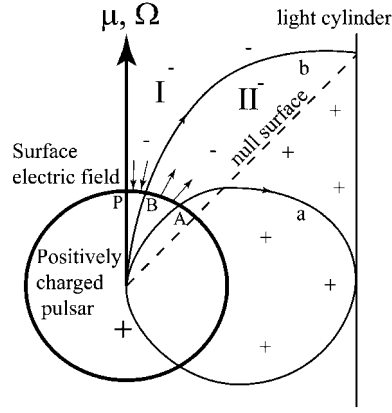


**Fig. 1** Sketch of the magnetic field line, electric field line, and magnetospheric charge distribution for an *aligned* pulsar. Line ‘a’ is the last open magnetic field line. Line ‘b’ is the *critical field line*. Region ‘I’: with a boundary of lines labelled ‘b’, and Region ‘II’: between lines ‘a’ and ‘b’. If the potential of line ‘b’ equals to that of interstellar medium, then the potential is positive within Region ‘II’ and negative within Region ‘I’.

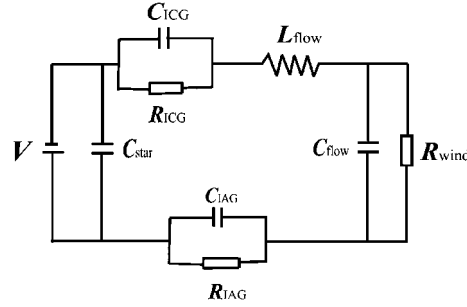


**Fig. 2** An equivalent circuit of pulsar magnetosphere. An electromotive source connected with other parts in series corresponding to the ICG, IAG, the outer gap (which is not essential in the model and thus not shown in the figure) and the pair-plasma wind. The current is determined by the power voltage  $V$ . “ $R$ ” stands for plasma resistance effects if a spark happens, mainly the losses of relativistic particles. “ $C$ ” represents the gap capacitance effects if there is a potential drop on the gap. “ $L$ ” describes the electromagnetic characteristic of flow.

these gaps could be simulated by a parallel connection of a resistor and a capacitor, connected to the other parts in series (as shown in Fig. 2).

In Figure 2, the power of the star is equivalently modelled by the voltage  $V$  and capacitance  $C_{\text{star}}$ . The star is magnetized and possesses an interior electric field,  $\mathbf{E}$ , which satisfies

$$\mathbf{E} + \frac{\boldsymbol{\Omega} \times \mathbf{r}}{c} \times \mathbf{B} = 0, \quad (1)$$

where  $\boldsymbol{\Omega}$  is the angular velocity of the star rotating around the dipole rotation axis, related to the rotating period  $P$  by  $P = 2\pi/\Omega$ . The magnetosphere of a rotating isolated-pulsar is thus generally concluded to be powered by an electric source with a certain potential drop between the polar

angle  $\theta_B$  and  $\theta$  of

$$\phi = \frac{R^2 \Omega B}{2c} (\sin^2 \theta - \sin^2 \theta_B) \approx 3 \times 10^{16} R_6^2 B_{12} P^{-1} (\sin^2 \theta - \sin^2 \theta_B) \text{ Volts}, \quad (2)$$

where  $R_6 = R/(10^6 \text{ cm})$ ,  $B_{12} = B/(10^{12} \text{ G})$ , assuming the pulsar is magnetized homogeneously. According to the equation of dipolar field line,  $r = r_d \sin^2 \theta$  ( $r_d$  is the maximum polar radius), and the polar angle of null surface  $\theta_n = \cos^{-1}(\pm 1/\sqrt{3})$ , one can obtain  $\sin^2 \theta_B = (2/3)^{3/2} R/R_L$ , where the radius of light cylinder  $R_L \equiv c/\Omega = cP/(2\pi)$ . The capacitance of the star with radius  $R$  is, in ‘cgs’ units,

$$C_{\text{star}} = 9 \times 10^{-21} R \text{ Farads}. \quad (3)$$

The electric flow process in a magnetosphere can be equivalently mimicked by an antenna cable with capacitance  $C_{\text{flow}}$  and inductance  $L_{\text{flow}}$ , with values estimated by

$$C_{\text{flow}} \simeq \frac{1}{2} l \left( \ln \frac{r_2}{r_1} \right)^{-1} \quad (4)$$

and

$$L_{\text{flow}} \simeq 2l \ln \frac{r_2}{r_1}, \quad (5)$$

respectively,  $l$ ,  $r_1$ , and  $r_2$  being the length, and inner and outer radius of the cable. The path length of the electric current is  $l \sim \sqrt{3/2} r_L = 5.8 \times 10^7 P \text{ m}$ . Near the light cylinder, the ratio  $r_2/r_1 \sim (r_L + r_L/\sqrt{2})/r_L = 1.7$ ; but on the stellar surface, the ratio  $r_2/r_1 = (3/2)^{3/4} = 1.4$ . Both values are independent of  $P$ ,  $B$ , or other parameters, and so we simply choose  $r_2/r_1 = 1.5$  in this paper. One therefore comes to

$$C_{\text{flow}} \sim 7.2 \times 10^7 P \text{ Farads}, \quad (6)$$

and

$$L_{\text{flow}} \sim 4.7 \times 10^7 P \text{ Henries}. \quad (7)$$

In case there is enough binding energy of charged particles on the star’s surface, an RS-type (RS75) vacuum gap should exist near the polar cap, which can be the equivalent of a capacitor of two parallel slabs, with

$$C_{\text{RS}} = \frac{r_p^2}{4h} = 5.3 \times 10^4 R_6^3 P h_3^{-1} \text{ Farads}, \quad (8)$$

where  $r_p = R \sin \theta_p = 1.45 \times 10^4 R_6^{3/2} P^{1/2} \text{ cm}$  is the radius of the polar cap, the gap height  $h$  is a model dependent parameter,  $h_3 = h/(10^3 \text{ cm})$ . From the above definition of ICG and IAG, we obtain the total values of  $C_{\text{ICG}}$  and  $C_{\text{IAG}}$ , by a simple replacement.

For the curvature-radiation-induced and the resonant inverse-Compton-scattering-induced cascade models, the gap heights  $h$  could be (e.g., Zhang, Harding & Muslimov 2000)

$$h_{\text{cr}} = 5.4 \times 10^3 \rho_6^{2/7} B_{12}^{-4/7} P^{3/7} \text{ cm}, \quad (9)$$

and

$$h_{\text{ics}} = 2.79 \times 10^4 \rho_6^{4/7} B_{12}^{-11/7} P^{1/7} \text{ cm}, \quad (10)$$

where  $\rho$  is the radius of curvature of the field line,  $\rho_6 = \rho/(10^6 \text{ cm})$ . In Zhang et al. (2000) the surface temperature,  $T_s$ , is treated self-consistently (i.e., self-sustained polar cap heating), and the gap parameter is thus not dependent explicitly on  $T_s$ .

If the field lines which cross the light cylinder can not co-rotate, then the active region on the surface of the star is the polar cap, from polar angle 0 to  $\theta_p \simeq \sqrt{2\pi R/(cP)} = 1.45 \times 10^{-2} (R_6/P)^{-1/2}$ . In this case, the potential difference of the electrical source is

$$V_{\text{cap}} = -6.58 \times 10^{12} R_6^3 B_{12} P^{-2} \text{ Volts}. \quad (11)$$

Since the dominant source of rotation energy dissipation is through  $R_{\text{wind}}$ , we can estimate  $R_{\text{wind}}$  with

$$R_{\text{wind}} \simeq \frac{V_{\text{cap}}^2}{\dot{E}_{\text{rot}}} = 11M_1^{-1}R_6^4B_{12}^2\dot{P}_{15}^{-1}P^{-1} \text{ Ohms}, \quad (12)$$

where the rotation loss rate  $\dot{E}_{\text{rot}} = -4\pi^2 I \dot{P} / P^3$ ,  $I \sim 10^{45} M_1 R_6^2 \text{ g}\cdot\text{cm}^2$  is the moment of inertia for a neutron star with mass  $\sim M_1 M_\odot$ , radius  $\sim R_6 \times 10 \text{ km}$ , and period derivative  $\dot{P}_{15} = |\dot{P}|/10^{-15}$ . Compared with  $R_{\text{wind}}$ , the stellar resistance  $R_{\text{star}}$  is negligible due to the perfect conductivity of the star.

The potential drop of the outer gap, where no spark happens, corresponds to a resistor, which is presumed to be combined with the wind dissipation into the  $R_{\text{wind}}$  in Figure 2. In the magnet dipole radiation model, the field  $B$  and the spindown  $\dot{P}$  is connected by (e.g., Manchester & Taylor 1977)  $B_{12} = 3.2 \times 10^7 \sqrt{P\dot{P}}$ , we then have

$$R_{\text{wind}} = 11M_1^{-1}R_6^4 \text{ Ohms}. \quad (13)$$

For the potential drops of the inner gaps (ICG and IAG), when sparking provides the necessary charge to close the circuit, they should correspond to the resistors ( $R_{\text{IAG}}$  and  $R_{\text{ICG}}$ , shown in Fig. 2). When there is no sparking, the gap grows and they can be described by the capacitors ( $C_{\text{IAG}}$  and  $C_{\text{ICG}}$ , shown in Fig. 2).

Let us analyze the circuit in Figure 2. Although the electric power has a fixed potential supply, the current is changing due to the inner gap sparks. In this sense, the equivalent circuit description in this paper is not a simple DC circuit. Because of the erratic sparking, the resistance  $R_{\text{RS}}$  could be taken as the sum of many sinusoidal functions of time,  $R_{\text{RS}} = \sum_{n=0}^{\infty} R_n \sin n\omega t$ . The electric current between arbitrary points  $M$  and  $N$  in the circuit can also be in this form,  $I_{\text{MN}} = \sum_{n=0}^{\infty} I_n \sin n\omega t$ .

According to the Kirchhoff's current and voltage laws, the complex impedances of parallel connection circuits composed of  $R_{\text{ICG}}$  and  $C_{\text{ICG}}$ ,  $R_{\text{IAG}}$  and  $C_{\text{IAG}}$ ,  $R_{\text{wind}}$  and  $C_{\text{flow}}$  are  $z_{\text{ICG}} = R_{\text{ICG}}/(1 + i\omega R_{\text{ICG}}C_{\text{ICG}})$ ,  $z_{\text{IAG}} = R_{\text{IAG}}/(1 + i\omega R_{\text{IAG}}C_{\text{IAG}})$ ,  $z_{\text{wind}} = R_{\text{wind}}/(1 + i\omega R_{\text{wind}}C_{\text{flow}}) + i\omega L_{\text{flow}}$ , respectively, where  $i = \sqrt{-1}$ ,  $\omega$  the angular frequency of electric current modulation. Defining  $z' \equiv z_{\text{ICG}} + z_{\text{IAG}} + z_{\text{wind}}$ , one obtains the total complex impedance to be

$$z_{\text{total}} = \frac{z'}{1 + i\omega z' C_{\text{star}}} \text{ Ohms}. \quad (14)$$

Let  $\omega = \omega_0$  when  $|z_{\text{total}}|$  is the smallest value. In this case, the potential drop between the inner vacuum gap is the highest. It is possible that there exists an oscillation with time scale  $\omega_0^{-1}$  in the circuit. We expect that some of the variations of radio intensity on different timescales could be hints of such circuit oscillations.

In case of  $C_{\text{ICG}} = C_{\text{IAG}} = L_{\text{flow}} = C_{\text{flow}} = 0$ , one has the total impedance  $z = R_{\text{ICG}} + R_{\text{IAG}} + R_{\text{wind}}$ . Physically this result represents a DC circuit model (Shibata 1991), where the total energy loss is generally assumed to be  $\dot{E}_{\text{rot}} \simeq 2\pi r_p^2 c \rho_{\text{GJ}} \cdot V_{\text{cap}}$ , with  $\rho_{\text{GJ}}$  the Goldreich-Julian density. This energy loss leads to a formula of calculating the pulsar magnetic field,  $B \simeq \sqrt{c^3 I P \dot{P} / (\pi^2 R^6)}$  (e.g., Manchester & Taylor 1977; Xu & Qiao 2001).

### 3 ARE PULSARS CHARGED ELECTRICALLY?

If the charged particles follow the Goldreich-Julian density distribution,  $\rho_{\text{GJ}}$ , they will be in balance with the electrostatic force. The equivalent ‘‘Poisson’’ equation in comoving frame then is (e.g., Beskin, Gurevich & Istomin 1993)

$$\nabla \cdot \mathbf{E} = 4\pi(\rho - \rho_{\text{GJ}}). \quad (15)$$

As mentioned by RS75, the electric field,  $\mathbf{E}_{\text{GJ}}$ , on the star's surface due to lack of charge density relative to the Goldreich-Julian density (e.g., for vacuum outside the star,  $\rho = 0$ ) is normal to

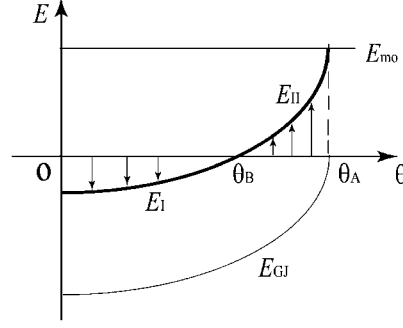


**Fig. 3** An illustration of the total electric field  $\mathbf{E}$  as a function of polar angle  $\theta$ .  $\mathbf{E}_{\text{GJ}}$  is due to the charge-separation in the pulsar magnetosphere, provided that the potential of line  $a$  is the same as the ISM.  $\mathbf{E}_{\text{mo}}$  is induced by the charges of the star. The total electric field (middle solid thick curve),  $\mathbf{E}_I$  and  $\mathbf{E}_{II}$  within the corresponding regions, could be a combination of  $\mathbf{E}_{\text{GJ}}$  (lower solid thin curve) and  $\mathbf{E}_{\text{mo}}$  (upper solid thin straight line).

the surface. The solution of RS75 (see its appendix I.b) for the electric field on the surface is  $E_s = -2\Omega B h/c < 0$ , which is equivalent to choosing the potential of the field line  $a$  to be the same as that of the ISM,  $\phi_A = 0$ . From Equation (15), one can also find generally the surface electric field  $E_{\text{GJ}} < 0$  in both *Regions* I and II, as shown in Figure 3.

When the potential of the line  $b$  is zero, as mentioned above, the direction of the electric field vector within *Region* I,  $\mathbf{E}_I$ , is inward while that in *Region* II,  $\mathbf{E}_{II}$  is outward. How can one understand consistently this picture? Why should this be reasonable if one choose  $\phi_B = 0$ , rather than  $\phi_A = 0$ ? The answer could be that there must be positive charges on the star surface which increases the potential of the star. These charges provide a monopole electric field  $\mathbf{E}_{\text{mo}}$ , which combines with  $\mathbf{E}_{\text{GJ}}$  to form the total electric field, as the shown by  $\mathbf{E}_I$  and  $\mathbf{E}_{II}$  in Figure 3.

The electricity induced by the charges on the star's surface is so high that the electric field is reversed across *Region* 'II' when the electric field of the star itself and the field caused by the charged particles are combined. Therefore, current can flow out and come back in the magnetosphere to close the pulsar's generator circuit. Reversing the argument, the increased electric field supports our assumption that the potential of line 'b' is zero.

Provided that two conditions are satisfied (first, the star has positive charges on the surface; secondly, the potential of the line 'b' is zero), the increase of the star's potential relative to that of ISM can be estimated to be of the order of the potential drop between 'A' and 'B' (from Eq. (2))

$$V_{\text{star}} \sim \phi_A - \phi_B = \frac{3 \times 10^{16} R_6^2 B_{12}}{P} (\sin^2 \theta_A - \sin^2 \theta_B) \approx \frac{3 \times 10^{12} R_6^3 B_{12}}{P^2} \text{ Volts.} \quad (16)$$

From Equations (3) and (16), the total charge  $Q$  on the star's surface is

$$Q = V_{\text{star}} \times C_{\text{star}} \approx \frac{3 \times 10^{-3} R_6^4 B_{12}}{P^2} \text{ Coulombs.} \quad (17)$$

Since the magnetic field  $B \sim \sqrt{P\dot{P}}$ , one has  $Q \sim \sqrt{\dot{P}/P^3} \sim \dot{E}_{\text{rot}}^{1/2}$ , where the rotation energy loss rate  $\dot{E}_{\text{rot}} \sim \Omega\dot{\Omega}$ . Observationally, the X-ray luminosity can be a function of the spin-down energy loss for all rotation-powered pulsars,  $L_x \sim \dot{E}_{\text{rot}}$  (Becker & Trümper 1997); but the  $\gamma$ -ray luminosity  $L_\gamma \sim \dot{E}_{\text{rot}}^{1/2}$  (Thompson 2003). One can also note that the energetic  $\gamma$ -ray luminosity is proportional to the electric charge  $Q$ , rather than to  $\dot{E}_{\text{rot}}$ .

Three quantities (mass  $M$ , angular momentum  $L$ , and charge  $Q$ ) are used to describe completely a black hole. The collapse of an evolved massive star might form temporally a rotating

magnetized pulsar, and then a black hole. It is possible that a pulsar would be charged with  $Q$  before a Kerr-Newman black hole forms finally. The black hole charge depends on the way of its formation, and may be proportional to  $B/P^2$ . This scenario could be tested if Kerr-Newman black holes are discovered.

One thinks conventionally, according to Equation (15), that *no* acceleration (e.g.,  $E_{\parallel} = 0$ ) occurs if  $\rho = \rho_{\text{GJ}}$  in pulsar magnetosphere. We note, however, that this conclusion is valid only if *no* solenoidal force field appears. In other words,  $E_{\parallel} \neq 0$  though  $\rho = \rho_{\text{GJ}}$  if one adds any solenoidal force field in the magnetosphere. A charged pulsar contributes a solenoidal electric field, which results in an acceleration near the pulsar (which decays as  $1/r^2$ ). In the close field line region, this electric field causes a re-distribution, so that  $E_{\parallel} = 0$ . In the open field line region, this field accelerates particles (for *aligned* pulsars, to accelerate negative particles in *Region I*, and positive particles in *Region II*; see Fig. 1). Certainly, an extra acceleration due to  $\rho \neq \rho_{\text{GJ}}$  exists too. As demonstrated in Figure 3, a very large acceleration may exist near the last open field lines, which could be favorable to the high energy emission in the caustic model (Dyks & Rudak 2003). An outer gap may not be possible if particles can flow out freely either from the surface (for negligible binding energy) or from the pair-formation-front (for enough binding energy) of a charged pulsar.

#### 4 LOW-MASS BARE STRANGE STARS

From above analysis, a pulsar's charge can be estimated through Eq.(17) if the quantities  $R$ ,  $B$  and  $P$  are known. What is the implication of charged pulsars? It is found in this section that millisecond pulsars may have small radii if the radio luminosity is proportional to the charge. Pulsars can be bare strange stars, and some of them can be of low-mass (Xu 2005). Due to the color self-confinement of quark matter, the density of low-mass bare quark star is roughly homogeneous, and its mass would be

$$M_{\text{QS}} = \frac{4}{3}\pi R^3(4\bar{B}) = 0.9R_6^3\bar{B}_{60}M_{\odot}, \quad (18)$$

where the bag constant  $\bar{B} = 60\bar{B}_{60} \text{ MeV fm}^{-3}$  (i.e.  $1.07 \times 10^{14} \text{ g cm}^{-3}$ ). For a star with pure dipole magnetic field and a uniformly magnetized sphere, the magnetic moment is

$$\mu = \frac{1}{2}BR^3. \quad (19)$$

If the magnetized momentum per unit mass is a constant  $\mu_{\text{m}} = (10^{-4} \sim 10^{-6})\text{G} \cdot \text{cm}^3 \cdot \text{g}^{-1}$ , the magnetic moment is (Xu 2005)

$$\mu = \mu_{\text{m}}M. \quad (20)$$

Combing Equations (18)–(20), one can obtain the magnetic field strength

$$B = 1.8 \times 10^{-18} \mu_{\text{m}} \bar{B}_{60} M_{\odot}. \quad (21)$$

Therefore, for a low-mass bare strange star, if the values of its period  $P$ , radius  $R$  (or the mass  $M_{\text{QS}}$ ), and the polar magnetic field  $B$  (or the parameter  $\mu_{\text{m}}$ ) are all known, the total charges on the surface can be obtained from Equation (17).

*Can we find evidence for low-mass millisecond pulsars?* The pulsar's radius was assumed to be a constant in above sections. In fact, the radius should vary according as we are dealing with a normal neutron star or a strange quark star. The radius of bare strange stars can be as small as a few kilometers (even a few meters). Could one find any observational hints about the star radius? It is suggested that normal pulsars might be bare strange stars with solar masses, whereas millisecond pulsars are of low masses (Xu 2005). Can we show evidence for low-mass millisecond pulsars in the bare strange star model for pulsars? These are investigated, based on the observed pulsar data.<sup>4</sup> There are 1126 pulsars with  $P$ ,  $\dot{P}$  and radio luminosity  $L_{1400}$  (mJy kpc<sup>2</sup>) at 1400 MHz all known. The numbers of millisecond and normal radio pulsars are 35 and 1091, respectively, if their dividing line is at  $P = 15$  ms. Here we refer the 35 millisecond radio pulsars ( $P < 15$  ms) as *Sample I* and the 1091 normal radio pulsars ( $P > 15$  ms) as *Sample II*.

<sup>4</sup> <http://www.atnf.csiro.au/research/pulsar/psrcat/>

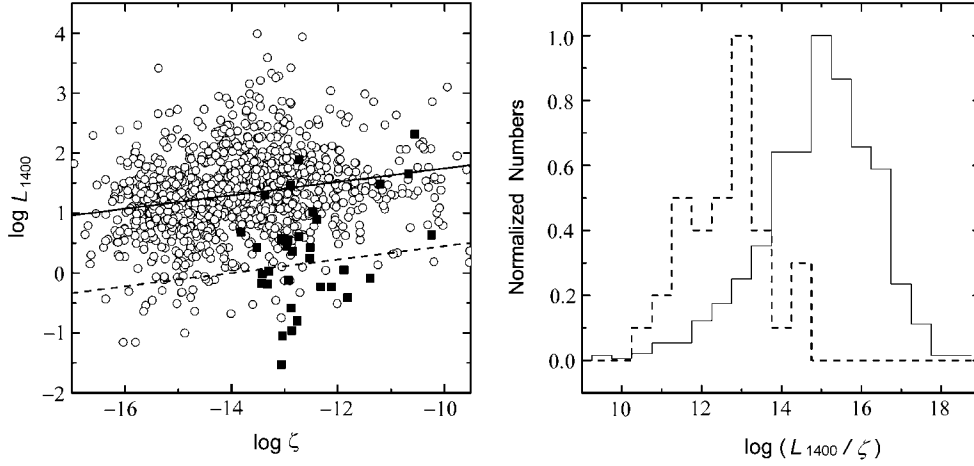


**Fig. 4** Left: Observed luminosity  $L_{1400}$  (mJy kpc<sup>2</sup>) at 1400 MHz as a function of  $\zeta$  for 1126 radio pulsars, where  $\zeta \equiv \frac{\dot{P}}{P^3}$ . The solid squares represent the millisecond radio pulsars (*Sample I*) with  $P < 15$  ms while the empty circles are the normal ones (*Sample II*) with  $P > 15$  ms. The solid line is the best least squares fit for *Sample II*, and the dash line is that for *Sample I*, with the slope assumed to be the same as *Sample II*. Right: Normalized number distribution of  $L_{1400}/\zeta$  for *Sample I* (dash step line) and *Sample II* (solid step line).  $L_{1400}/\zeta$  is only a function of pulsar radius according to Eqs. (22)–(25).

Assuming the pulsar radius is a variable, from Equation (17), one can obtain the pulsar's charge  $Q \sim R^4 \frac{B}{P^2} \sim R^4 (\frac{\dot{P}}{P^3})^{1/2}$  since the magnetic field strength  $B \sim \sqrt{P\dot{P}}$ . Defining  $\zeta \equiv \frac{\dot{P}}{P^3}$ , one comes to

$$\log Q \sim 4 \log R + \frac{1}{2} \log \zeta. \quad (22)$$

At the same time, the rotation energy loss rate  $\dot{E}_{\text{rot}} \simeq I\Omega\dot{\Omega} \sim R^5\zeta$ , where the rotational inertia of the star  $I \simeq \frac{2}{5}MR^2 \sim R^5$  (the star is assumed to be a homogeneous rigid sphere), i.e.,

$$\log \dot{E}_{\text{rot}} \sim 5 \log R + \log \zeta. \quad (23)$$

The correlation between  $L_{1400}$  and  $\zeta$  and the normalized number distribution of  $L_{1400}/\zeta$  are shown in Figure 4. One can see that, for a certain value of  $\zeta$ , the luminosity of a millisecond pulsar is lower than that of a normal pulsar.<sup>5</sup> For showing evidence for low-mass millisecond pulsars by this relation and distribution, we first give the best fit line by the least square method for the larger *Sample II*. Next, we assign the slope of fitting line for the smaller *Sample I* to be the same as that of *Sample II*. Third, we check the relation  $L \sim R$  separately on two assumptions,  $L = L(Q)$  (i.e.,  $L$  is only a function of  $Q$ ) and  $L = L(\dot{E}_{\text{rot}})$  (i.e.,  $L$  is only a function of  $\dot{E}_{\text{rot}}$ ). Finally, through comparing the intercepts of two fit lines, we can obtain the ratio of radius of *Sample I* to that of *Sample II*.

From the left panel in Figure 4, we find that the best fit line for *Sample II* is

$$\log L_{1400} = 2.86 + 0.11 \log \zeta. \quad (24)$$

Assigning the same slope for *Sample I* and defining the radius ratio of *Sample I* to *Sample II* as *Ratio I*, we find that the intercept of fit line for this sample is 1.56.

<sup>5</sup> A low-mass normal neutron star can not spin rapidly at a period of  $\sim$  ms. The inertia of a low-mass neutron star is  $\sim MR^2 \sim M^{1/3}$ . Therefore, this observation may not be explained by the suggestion that millisecond pulsars are low-mass normal neutron stars.

**Table 1** The radius and mass ratios with assigned slope of *Sample I* (*Ratio I*) and with assigned slope of *Sample II* (*Ratio II*). Radius ratio,  $R_I/R_{II}$ ; Mass ratio,  $M_I/M_{II}$ ; suffix I referring to millisecond pulsars; II, normal pulsars.

$L \sim Q$ relation	Radius <i>Ratio I</i>	Mass <i>Ratio I</i>	Radius <i>Ratio II</i>	Mass <i>Ratio II</i>
$L = lQ^m$	0.35	0.04	0.03	$2 \times 10^{-5}$
$L = k\dot{E}_{\text{rot}}^n$	0.18	$6 \times 10^{-3}$	0.004	$5 \times 10^{-8}$

If  $L = lQ^m$ , with ( $l$ ,  $m$  two constant parameters), then from Equations (22) and (24), we obtain the *Ratio I*, at 1400 MHz, shown in the second column, first line of Table 1. In the same way, if  $L = k\dot{E}_{\text{rot}}^n$  with  $k$ ,  $n$  constant parameters, then from Equations (23) and (24), we obtain the *Ratio I*, shown in the second column, second line, of Table 1. In addition, the best fit line for *Sample I* is

$$\log L_{1400} = 4.73 + 0.35 \log \zeta. \quad (25)$$

Assigning the same slope as for *Sample II*, we find that the intercept of the fit line for this sample is 6.04. Then, for  $L = lQ^m$  or  $L = k\dot{E}_{\text{rot}}^n$ , one obtains the ratios of  $R_I/R_{II}$  (*Ratio II*) shown in the fourth column of Table 1. The ratios of the mass of millisecond pulsars to that of normal pulsars,  $M_I/M_{II}$ , can also be calculated from Equation (18); the results are also shown in Table 1.

From the right panel in Figure 4, it is evident that the values of  $L_{1400}/\zeta$ , as a function of pulsar radius, include two peaks, the higher one (larger radius) for normal pulsars, and the lower one (smaller radius) for millisecond pulsars.

In sum, the radii of *Sample II* are always larger than those of *Sample I*, which gives evidence that millisecond pulsars have smaller radii and masses than those of normal radio pulsars. Especially, from the right panel in Figure 4, we see that the normalized distributions of  $L_{1400}/\zeta$  for *Sample I* and *Sample II* are separately clustered around about 13 and 15. This two-peak structure gives roughly the same result and supports the evidence for low-mass millisecond pulsars. If one thinks that normal pulsars are bare strange stars with mass  $\sim M_\odot$ , the mass of millisecond pulsars can be as low as  $\sim 10^{-2}M_\odot$ , or even more lower.

## 5 CONCLUSIONS AND DISCUSSION

We assume the pulsar magnetosphere to have a global current which starts from the star, runs through the inner core gap, the wind, the outer gap and the inner annular gap, and returns to the star. Moreover, we study the characteristics of the four circuit elements: the electromotive source, inner core gap, inner annular gap, and the outer gap and wind. It is emphasized that the potential of the *critical field lines* is equal to that of interstellar medium. We find, in this case, that an aligned pulsar, whose rotation axis and magnetic dipole axis are parallel, should be positively charged for the pulsar's generator circuit to be closed. The current flows out through the light cylinder and then flow to the stellar surface along the open magnetic field line. One can extend this study for oblique pulsars. For an orthogonal pulsar, Beskin & Nokhrina (2004) have argued that the current may flow between the regions of closed and open field lines.

There are five independent parameters to describe completely the dynamics of a pulsar magnetosphere with a dipole field and a uniform density of the star. They are the radius  $R$ , the mass  $M$  ( $\simeq 16\pi\bar{B}R^3/3$  in case of bare strange stars, with  $\bar{B}$  the bag constant), magnetic strength  $B$  (or magnetic moment  $\mu \sim BR^3$ ), period  $P$ , and the inclination angle  $\alpha$ . Typical parameters for radio pulsars are:  $R \sim 10^6$  cm,  $M \sim 1.4M_\odot$ ,  $P \sim (10^{-3} - 1)$  s, and  $B \sim 10^8 - 10^{12}$  G. There is no solid observational evidence for these parameter values being really *typical*. In case that pulsars are bare strange stars (probably with low masses), some of the above values may not be representative, and some parameters may be related to each other (Xu 2005). The statistics between the radio luminosity and pulsar's electric charge (or the spindown power) may hint that millisecond pulsars could be low-mass bare strange stars.

We have only modeled the magnetospheric circuit for aligned pulsars. However, this does not mean that our model would not be applicable to the more general case of oblique pulsar. In a

previous calculation (fig. 2 of Qiao et al. 2004), it is shown that the geometry of the annual region is not changed quantitatively when the inclination angle varies from  $0^\circ$  to  $75^\circ$ . We may expect that the results presented in this paper will not change significantly for oblique rotators, but detailed considerations on the issues are necessary in future work.

**Acknowledgements** The authors thank the members of the pulsar group of Peking University for helpful discussion, and sincerely acknowledge the helpful comments and suggestions from an anonymous referee. This work is supported by the NSFC (Nos. 10573002, 10373002) and the Key Grant Project of Chinese Ministry of Education (G305001).

## References

- Arons J., Scharlemenn E. T., 1979, *ApJ*, 231, 854  
Becker W., Trümper J., 1997, *A&A*, 326, 682  
Beskin V. S., Gurevich A. V., Istomin Y. N., 1993, *Physics of the Pulsar Magnetosphere*, Cambridge: Cambridge Univ. Press  
Beskin V. S., Nokhrina E. E., 2004, *Astronomy Letters*, 30, 685  
Cheng K. S., Ho C., Ruderman M., 1986, *ApJ*, 300, 500  
Dyks J., Rudak B., 2003, *ApJ*, 598, 1201  
Goldreich P., Julian W. H., 1969, *ApJ*, 157, 869  
Harding A. K., Muslimov A. G., 1998, *ApJ*, 508, 328  
Hewish A., Bell S. J., Pilkington J. D. et al., 1968, *Nature*, 217, 709  
Kim H., Lee H. M., Lee C. H., Lee H. K., 2005, *MNRAS*, 358, 998  
Manchester R. N., Taylor J. H., 1977, *Pulsars*, Freeman: San Francisco  
Melrose D., 2004, in: *Young Neutron Stars and Their Environments*, IAU Symp. 218, eds F. Camilo, B. M. Gaensler, San Francisco, p.349  
Qiao G. J., Lee K. J., Wang H. G., Xu R. X., Han J. L., 2004a, *ApJ*, 606, L49  
Qiao G. J., Lee K. J., Zhang B., Xu R. X., Wang H. G., 2004b, *ApJ*, 616, L127  
Ruderman M. A., Sutherland P. G., 1975, *ApJ*, 196, 51  
Shibata S., 1991, *ApJ*, 378, 239  
Sturrock P. A., 1971, *ApJ*, 164, 529  
Subharthi R., Manuel M., José P. S. L. et al., 2004, *Braz. J. Phys.*, 34, 310  
Thompson D. J., 2003, in: *Cosmic Gamma Ray Sources*, eds K. S. Cheng, G. E. Romero, Kluwer ASSL Series (astro-ph/0312272)  
Wang H. G., Qiao G. J., Xu R. X., 2003, *ChJAA*, 3, 443  
Xu R. X., 2003a, in: *Stellar astrophysics — a tribute to Helmut A. Abt*, eds K. S. Cheng, K. C. Leung & T. P. Li, Kluwer Academic Publishers, p.73 (astro-ph/0211563)  
Xu R. X., 2003b, *ChJAA*, 3, 33  
Xu R. X., Qiao G. J., 2001, *ApJ*, 561, L85  
Xu R. X., 2005, *MNRAS*, 356, 359  
Zhang B., Harding A. K., Muslimov A. G., 2000, *ApJ*, 531, L135